

ASSESSMENT OF GAMMA–THETA TRANSITIONAL MODEL FOR LAMINAR-TURBULENT TRANSITION PREDICTION IN SUPERCRITICAL AIRFOILS

Ernesto Benini*, Rita Ponza

*Author for correspondence

Department of Mechanical Engineering,

University of Padova,

Padova – I-35131

Italy,

E-mail: ernesto.benini@unipd.it

ABSTRACT

A numerical study on the capability of the γ - θ turbulence model for predicting the laminar/turbulent transition in the boundary layer developing around a supercritical airfoil (NLR 7301) is described. The range in the Mach number explored is [0.3, 0.825], thus covering a fully transonic flow regime. For this purpose, a CFD solver (ANSYS CFX[®]) is used on a hybrid structured-triangular grid, where an accurate mesh setup of the wall boundary layer was performed in order to ensure (i) a value of y^+ less than 6 everywhere and (ii) a number of boundary layer rows within the physical boundary layer no less than 4. Results obtained are compared to the experimental data described in the open literature and discussed in detail. Despite the various sources of uncertainty affecting the experimental data, the results regarding the transition location revealed a very good model predictive capacity for low-to-medium Mach numbers (Mach<0.6), while exhibiting a less satisfactory ability in the transonic regime (Mach>0.6). In this case, prediction of transition location on both sides of the airfoil is still accurate even if the correlation on the pressure distributions gets poorer.

INTRODUCTION

Prediction of turbulence transition in wall boundary layers has been of major interest for almost all aerodynamic designers since ever. Being restricted to the research and academic communities for a long time, this problem has now become quite popular in industry as well, where commercial CFD tools are today used routinely with more and more increased effectiveness. As a consequence, considerable attention is directed, even in the scientific community, toward new implementations of CFD tools in commercial solvers, especially in order to critically assess their validity and provide industry with the correct information about their usage.

Predictive γ - θ laminar-turbulent model developed by Menter et al. [1,2] is probably one of the first turbulence transition tools for commercial CFD and is embedded into the latest release of the ANSYS CFX[®] software. According to the authors, it is suitable for low-to-medium Mach number flows, both developing around bodies in an open domain (e.g. airfoils) or within bounded walls (e.g. in turbomachinery) and delivers good performance on 2D-3D unstructured grids on both single-processor and parallel machines. Such model is actually an evolution of the original k - ω SST formulations by Menter [3-5] in that a new correlation-based transition model has been developed which is based strictly on local variables. The model is based on two transport equations, one for intermittency and one for the transition onset criteria in terms of momentum thickness Reynolds number. The proposed transport equations do not attempt to model the physics of the transition process (unlike, e.g., turbulence models) but form a framework for the implementation of correlation-based models, which are not yet of public domain, into general-purpose CFD methods. For a detailed description of the model the reader is referred to Menter et al. [1,2], where both theoretical formulation and some of the basic test cases used for model validation are described.

In this paper, an assessment of the γ - θ model is presented on a rather challenging test case, a thick, supercritical airfoil under low-to-transonic flow regimes, where the boundary layer is subject to rather strong adverse pressure gradients on the suction side even at zero incidences. The capabilities of the model are evaluated by comparing the computed vs. experimental values of the transition point over both the suction and the pressure side of the airfoil, as well as by assessing the discrepancy between measured and calculated overall drag and lift coefficients. A comparison between predicted and measured pressure distributions is finally provided.

NOMENCLATURE

- M = Mach number
- Re = Reynolds number
- T_0 = Total temperature in the far field flow, K
- T_{inf} = Static temperature in the far field flow, K
- p_{inf} = Static pressure in the far field flow, Pa
- p_{din} = Dynamic pressure in the far field flow, Pa
- CL = Lift coefficient
- CD = Drag coefficient
- x = Airfoil abscissa, m
- c = Airfoil chord, m
- C_p = Pressure coefficient
- α = Angle of attack, deg
- μ = Dynamic viscosity, kg/ms
- ρ = Density, kg/m³

THE CASE STUDY

A test case was considered to check the capabilities of the transitional $\gamma-\theta$ model. This consists in the 2D airfoil known as NLR 7301 [6], an aft-loaded shock-free supercritical airfoil developed and studied at the NLR laboratories, for which an extensive documentation exists regarding accurate measurement of the transition point at various Mach number flow regimes, while the Reynolds number is almost fixed. Actually the profile was experimentally investigated both with free and imposed transition. This test case was also selected because it represents a rather extreme specimen of thickness, a condition which permits to better evaluate the transition model capabilities under challenging flow conditions characterized by strong adverse pressure gradients occurring on the airfoil suction side. In fact, it appeared from the tests that, even at subcritical conditions, and both in free and fixed transition, the boundary layer on either the upper or the lower surface is stressed to limits. As a result, the effects of variations in transition position and transition fixing are rather dramatic. Moreover, it is worth noting that, when transition was left free, it generally occurred through a laminar separation bubble which is often reflected in the pressure distribution; on the other hand, with fixed transition at 30% chord the trip caused a local perturbation of the pressure distribution.

The airfoil geometry is depicted in Figure 1, the complete set of profile coordinates is given elsewhere. The airfoil chord length is 0.18 m and the thickness to chord ratio is 16.5%. A finite trailing edge thickness is obtained by cutting-off the theoretical airfoil at 98.5% chord.

The airfoil was tested at the NLR Pilot closed-circuit Wind Tunnel, where an excellent two-dimensional flow field was realized, having a rectangular test section (0.55 m height x 0.42 m width). Reference static pressure in the tunnel was taken 3.6 chords upstream of the model. The type of measurements consisted in surface pressure data (from which lift and pitching moments were derived), wake Pitot pressure data for determining the drag, surface flow visualization and flow field visualization. Surface pressure measurements were carried out by means of 0.25 mm diameter pressure holes (Figure 1), staggered around the center line at various chordwise positions. Wake measurements were performed using a wake rake of 69

tubes located 0.8 chords downstream of the profile trailing edge. No boundary layer measurements were carried out. Flow visualization was conducted using shadowgraph pictures and the detection of transition position was realized by means of a sublimation technique (using acenaphtene).

During the tests, the Mach number was changed from 0.3 to 0.85 while the Reynolds number was fixed at about $2 \cdot 10^6$. As already mentioned, the transition could be either free or fixed, the latter being possible by using glass beads bands of 2 mm width at 30% chord on upper and lower surface.

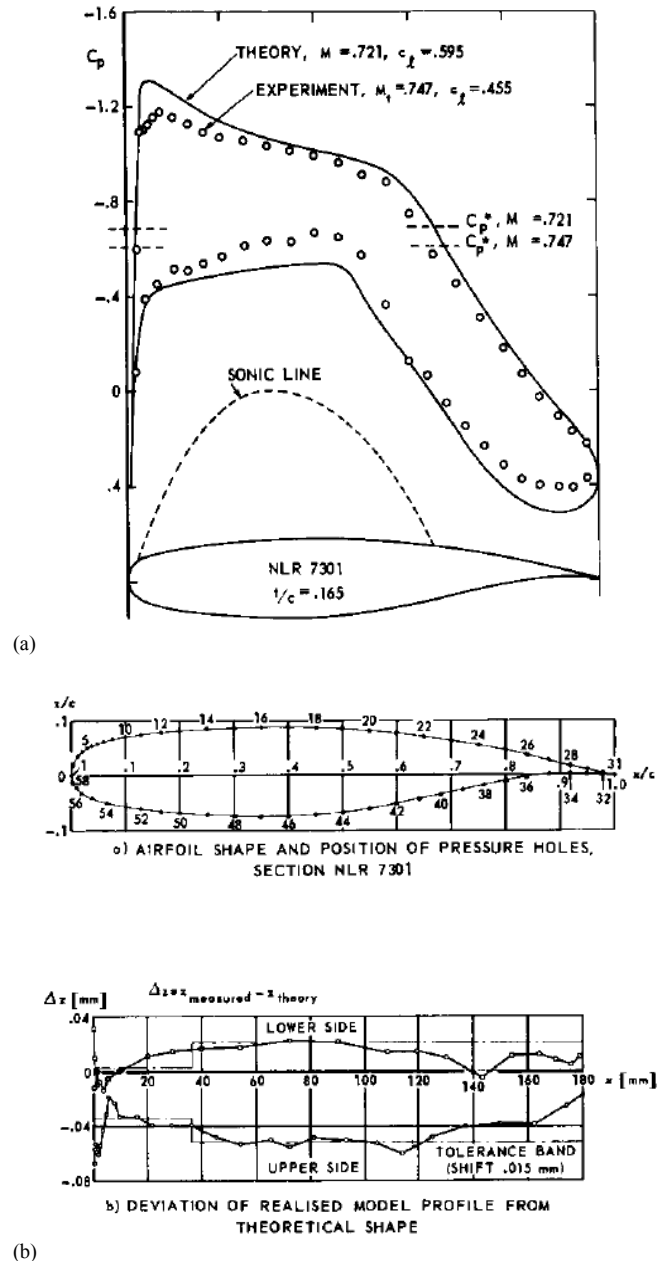


Figure 1 Airfoil geometry and pressure coefficient distribution (a); position of static pressure holes and deviation of realized model from theoretical shape (b) (from AGARD [6])

CFD COMPUTATIONS

A campaign of CFD computations using the commercial RANS solver CFX ANSYS© was performed on the NLR airfoil applying the same boundary conditions used in the experiments with the aim of validating the transitional model. The position of the transition, the values of both the lift and drag coefficients and the pressure coefficient distribution were computed at various Mach numbers while keeping the angle of attack close to 0°.

Computational grids around the profile were built as follows. A high-quality structured mesh was created close to the airfoil surface with the purpose of better capturing the surface boundary layer and to obtain y^+ values compatible with the recommended ones beyond the use of the γ - θ model (around 1). It is worth remembering that, if the y^+ parameter violates the above mentioned constraint, the wall shear stress is not satisfactorily calculated, thus leading to fairly incorrect results. In Table 1 the characteristic data of the grid boundary layer around the airfoil are reported.

Outside the boundary layer, a triangular non-structured grid was created using proper size functions (in particular a growth rate of 1.05 and a maximum size of 22.2 mm were adopted). This mesh made it possible to ensure that the number of grid layers inside the physical boundary layer was typically from 4 at the airfoil leading edge to 20 at the trailing edge. This is fundamental for describing the velocity profile and its derivatives inside the physical boundary layer with reasonable accuracy, since this has a remarkable impact on the numerical evaluation of the momentum-thickness Reynolds number $Re_{\theta_t} = \rho U \theta_t / \mu$, which in turns influences the transition onset. In Figure 2 (a) a view of the global mesh is depicted, while in Figure 2 (b),(c) some details are shown of the grid boundary layer around the airfoil near the leading edge and the trailing edge regions respectively.

The boundary conditions were as follows: while a no-slip condition was adopted for the airfoil walls, a pressure inlet condition was applied at the domain inlet while at the domain outlet a pressure outlet value was imposed, the actual values of both depending on the Mach and Reynolds numbers being simulated (Figure 3). The turbulence intensity was not clearly defined in the AGARD report; practical considerations about the type of wind tunnel used in the experiments suggested that low turbulence intensity is to be expected. Therefore, turbulence levels ranging from 1 to 4% were investigated. The complete simulation matrix including the pertinent set of boundary conditions is given in Table 2. The actual angle of attack α for the two-dimensional case is also reported⁶, in which a semi-empirical correlation was used to evaluate the wing downwash effect with varying Mach number. Only the case of free transition was simulated.

In order to effectively initialize the flow domain for a robust transitional solution, thus avoiding the occurrence of code divergence, an iterative solution strategy was adopted as follows. For each step, a converged solution where a normalized residual on the continuity equation less than $5 \cdot 10^{-5}$ was obtained:

- 1) Boundary conditions were applied to a viscous fluid (air) having constant density; the turbulence model used is the SST transitional since the first iterations, with a second order discretization solution scheme and under-relaxation factors equal to 0.3 on all the quantities;
- 2) Next, the fluid was switched to an ideal gas model, still using under-relaxation factors equal to 0.3;
- 3) Finally, the under-relaxation factors were switched to the default values, while lift and drag coefficients were monitored as functions of the number of iterations.

The stop criterion was established when either the normalized residuals fell under the limit above or the monitored quantities reached a stable pattern with increasing number of iterations.

Table 1 Grid boundary layer (BL) data

Number of grid points on the airfoil	348 on upper side 348 on lower side
Distribution of grid points on airfoil	Doubled sided successive ratio 1.01
BL number of rows	40
BL first row thickness	0.556 mm
BL growth factor	1.05

Table 2 Simulation matrix and pertinent boundary conditions

M	Re	T_0 [K]	T_{inf} [K]	$\mu \cdot 10^5$ [kg/ms]
0.3	1,200,000	313	307	1.706
0.5	1,700,000	313	298	1.829
0.6	1,900,000	313	292	1.845
0.65	2,000,000	313	289	1.834
0.7	2,100,000	313	285	1.813
0.724	2,200,000	313	283	1.757
0.747	2,200,000	313	282	1.779
0.774	2,200,000	313	279	1.804
0.8	2,300,000	313	277	1.745
0.825	2,300,000	313	275	1.761

M	ρ [kg/m ³]	P_{inf} [Pa]	P_{din} [Pa]	α [deg]
0.3	1.0787	95191	6133	0.4
0.5	0.9984	85419	15906	0.4
0.6	0.9479	79439	21885	0.38
0.65	0.9209	76280	25044	0.38
0.7	0.8928	73048	28277	0.39
0.724	0.8791	71478	29846	0.38
0.747	0.8658	69967	31358	0.2
0.774	0.8500	68187	33137	0.25
0.8	0.8346	66471	34853	0.4
0.825	0.8198	64822	36502	0.6

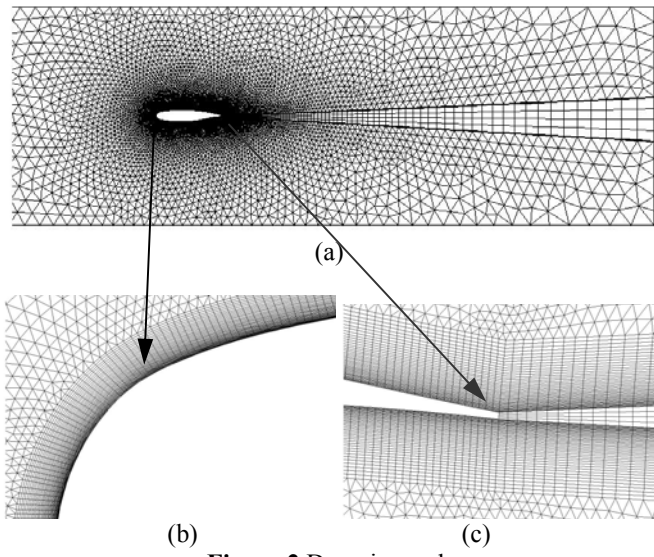


Figure 2 Domain mesh

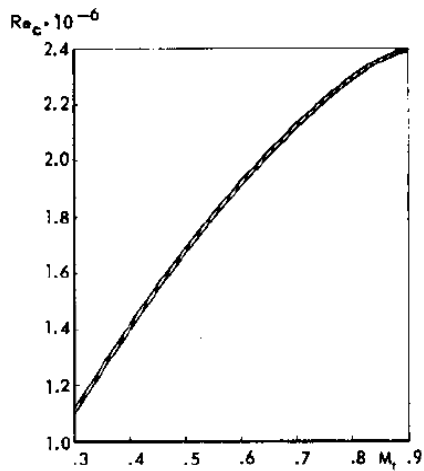


Figure 3 Reynolds number based on chord length as function of test Mach number (from AGARD [6])

RESULTS

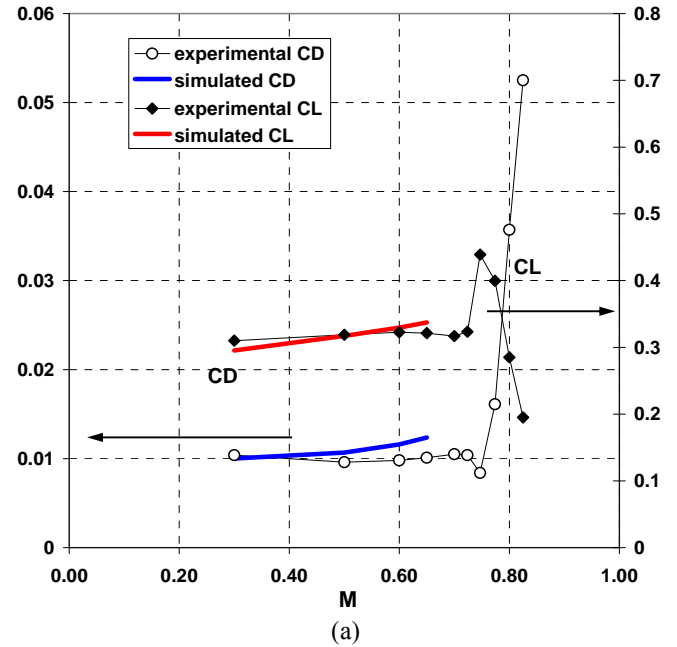
Prior to the extraction of the following data, a grid sensitivity analysis was performed. In particular three grids were analyzed, from a coarse (about 25,000 elements) to a fine configuration (about 100,000 elements). An intermediate grid of 80,000 elements was also studied (to which the grid parameters of Table 1 are referred). Since no appreciable modifications were noticed regarding the airfoil performance when passing from the fine to the intermediate grid, the latter was actually adopted as the definitive configuration to which the final results refer.

Results at low-to-medium subsonic Mach numbers

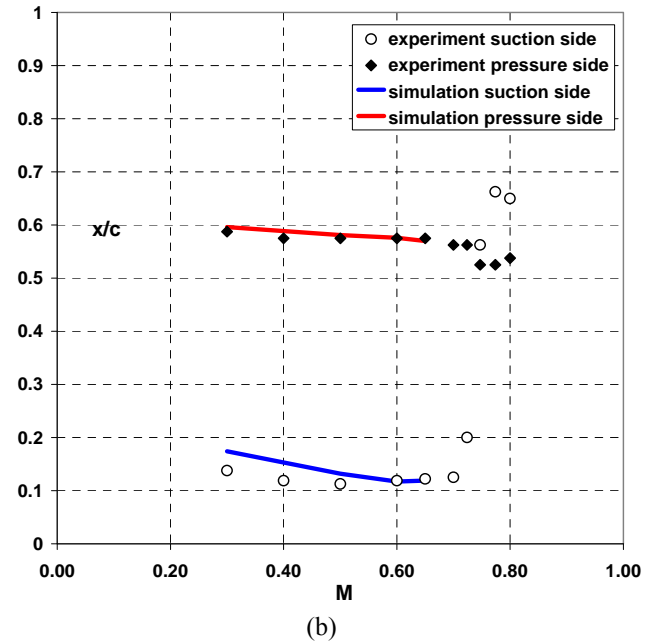
This section refers to computations carried out using Mach numbers varying in the range from 0.3 to 0.65. It is worth

recalling that the following results refer to the case where free transition was studied in the experiment.

Figure 4 (a) compares the experimental and numerical values of the lift and drag coefficients as a function of the Mach number when the actual angle of attack is as specified in Table 2. All the results refer to a turbulence intensity of 1.25%.



(a)



(b)

Figure 4 Lift and drag coefficients as a function of the Mach number in the range $0.3 \leq M \leq 0.65$ (a). Location of natural laminar/turbulent transition in the range $0.3 \leq M \leq 0.65$: comparison between experimental and computed values (b)

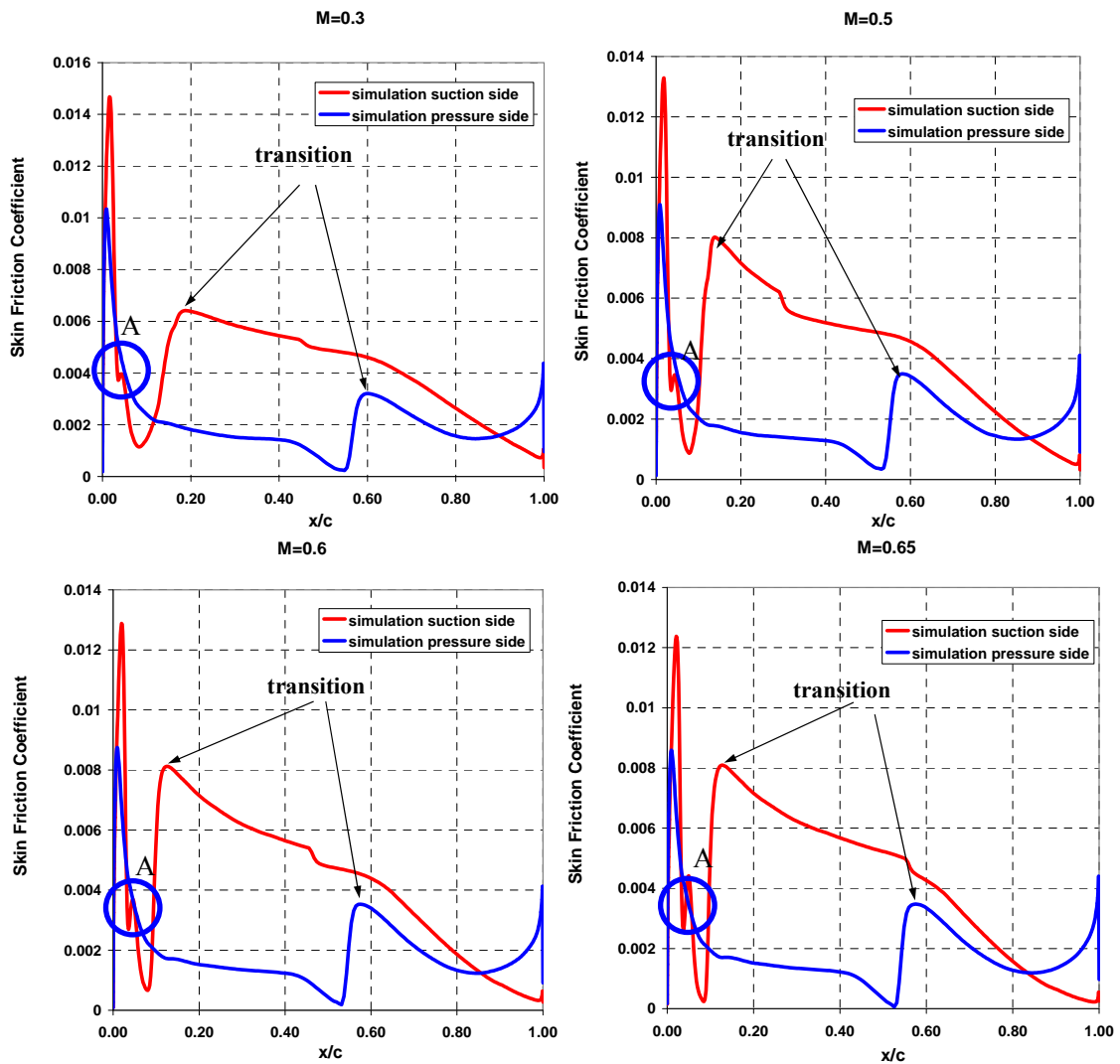


Figure 5 Skin friction coefficient distributions over the airfoil surface

In post-processing the numerical data, the drag coefficient was calculated by integrating the wall shear stresses onto the airfoil surfaces: this is implicitly done using the report forces command in the ANSYS© environment. This method gave the best predictions when compared to other well-known procedures (e.g. that based on momentum balance from inlet to outlet). The lift coefficient was calculated using the same procedure where pressure action is integrated on the airfoil surface. From the figure., a very good estimation of the drag coefficient can be registered at low Mach numbers (actually at $M=0.3$ data are almost overlapped); as the Mach number increases the numerical estimation gets poorer, the maximum discrepancy being in the order of 21% at $M=0.65$. However this prediction can be considered satisfactory overall, especially when compared to other well-known results in the open literature. A similar behavior is evidenced as far as the lift

coefficient is concerned, with a maximum error of 5% at $M=0.65$, while at $M=0.3$ the simulated CL is underpredicted by about 4%. As will be explained below, this lack of correlation is partially explainable by examining the pressure distribution on the airfoil as the Mach number increases.

Figure 4 (b) compares the experimental and numerical values of the non-dimensional abscissa of the natural transition point from laminar to turbulent. In the numerical simulations, the actual location for transition is identified in the position where a sudden increase in the skin friction coefficient is registered: actually, the transition was considered to occur at the local maximum of the skin friction coefficient, given that neither exact indications about experimental measurements are given [6], nor definite location of transition is physically identifiable.

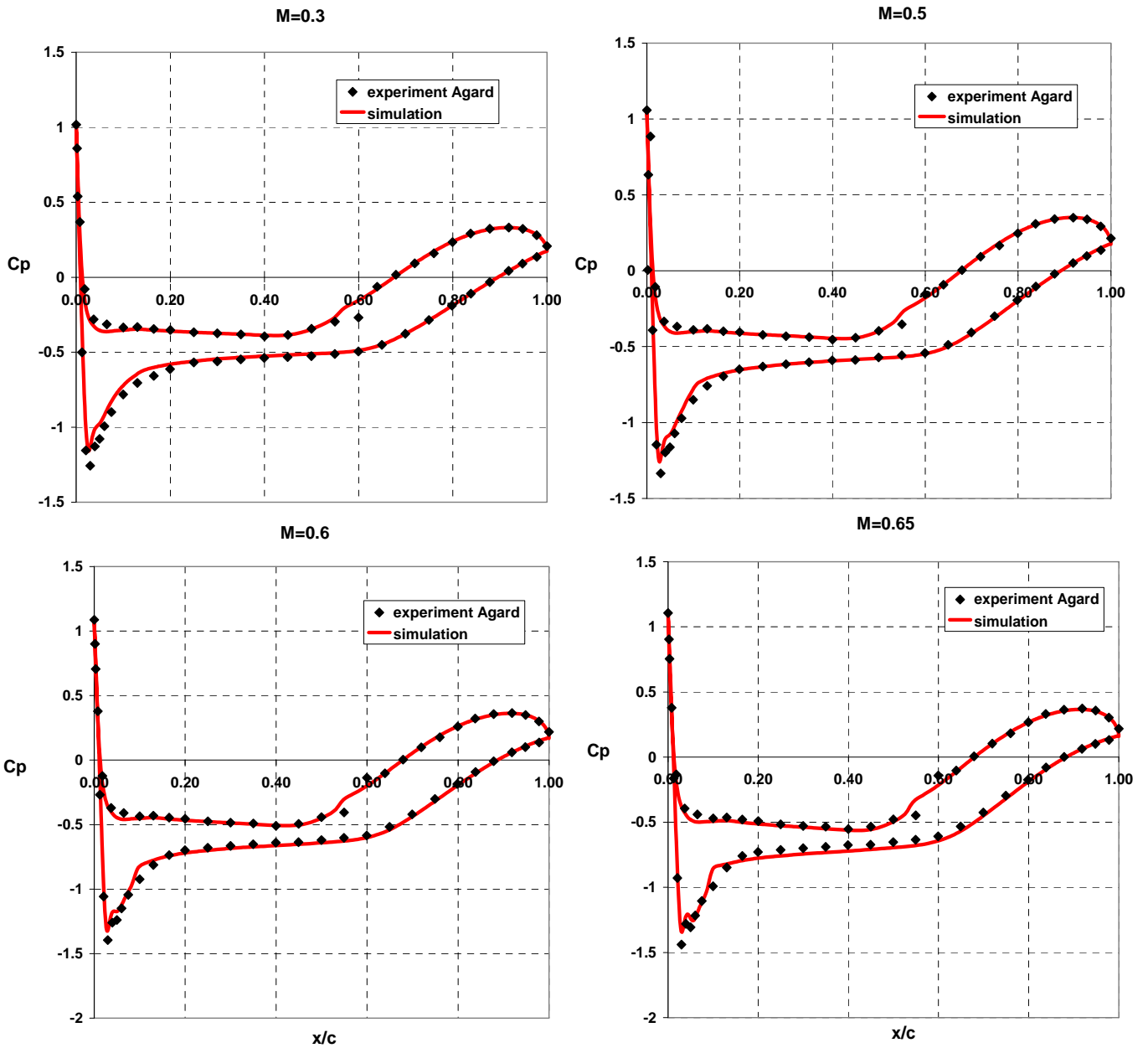


Figure 6 Pressure coefficient distributions over the airfoil surface in the range $0.3 \leq M \leq 0.65$

Figure 5 outlines the complete set of results obtained within the investigated Mach number interval. While post-processing numerical data, attention should be paid not to misread the real transition point by getting trapped into a misleading local peak (zone “A” in Figure 5) which typically occurs on the suction side near the airfoil leading edge, perhaps caused by numerical errors. From the Figure 5, a very good estimation of the transition location is highlighted on the airfoil pressure side, where the curve is rather flat with growing Mach numbers. As far as the suction side is concerned, the transition behavior is

qualitatively well captured, even if at the lowest Mach numbers the predicted transition onset occurs slightly more downstream than the experimental one.

The pressure coefficient distribution is outlined in Figure 6: data confirm the slight underprediction of lift coefficient at $M=0.3$, due to a somewhat higher pressure over the first 20% of the chord on the suction side, while justifying on the other hand a little overprediction at higher Mach, due to the slightly lower pressure over a significant portion of the airfoil suction side.

Results at medium-to-high transonic Mach numbers

This section refers to computations carried out in a higher range of transonic Mach numbers, from 0.7 to 0.825. Again, the following results refer to the case where free transition was studied in the experiment.

Figure 7 (top) compares the experimental and numerical values of the lift and drag coefficients as a function of the Mach number when the actual angle of attack is as specified in Table 2. All the results refer to a turbulence intensity of 1.25%.

As already stressed out before, the drag coefficient was calculated by integrating the wall shear stresses onto the airfoil surfaces, while the lift coefficient results from the integration of the pressure action on the airfoil. It is worth noting that for $M \geq 0.774$ a first order discretization solution scheme needed to be adopted for all the variables, otherwise the simulations did not converge: this obviously makes the solutions less accurate than a second order scheme would allow, however some useful qualitative indications could still be obtained.

While at $M=0.7$ the discrepancy of the predicted aerodynamic coefficients over the experiments is in the same order of that obtained at lower Mach numbers, with an error of +10% on the lift and +27% on the drag coefficient, at Mach higher than 0.7 the error gets higher and higher. However, despite the apparently poor correlation in the transonic region, the code is able to capture the overall airfoil behavior with varying Mach numbers, thus making it possible to obtain qualitative information on both the drag and lift trends. Specifically, a strong drag divergence with increasing Mach numbers is evidenced, even if it is anticipated with respect to the experimental one. Also the lift coefficient qualitative trend is captured very well, despite being translated toward lower Mach number values compared to the experimental ones: the curve exhibits a peak at $M=0.724$ and then rapidly drops down, while the drag suddenly grows. A more detailed investigation on the pressure coefficient distribution on the airfoil upper and lower surfaces can give a better insight into the reason for such a discrepancy (see later on).

In Figure 7 (bottom) the experimental and numerical values of the non-dimensional abscissa of the natural transition point from laminar to turbulent are compared. Again, the actual location for transition is identified in the position where a local maximum in the skin friction coefficient is registered. From this figure, a satisfactory qualitative estimation of the transition location is highlighted on both pressure and suction side of the airfoil. In particular, the sudden downstream shift of the transition on the suction side at divergence Mach number is captured. The transition location on the pressure side, while being rather flat at $M \leq 0.65$, shifts slightly upstream at higher Mach numbers, and reaches a local minimum at $M=0.774$: this is again very well captured by the simulations.

Figure 8 outlines the complete set of results obtained within the investigated Mach number interval. Again, while post-processing numerical data, attention should be paid not to misread the real transition point by getting trapped into a misleading local peak (zone "A" in the figure) which typically occurs on the suction side near the airfoil leading edge, perhaps caused by numerical errors.

The pressure coefficient distribution is outlined in Figure 9: as can be observed, correlation is very poor, and gets worse and worse as the Mach number increases. Furthermore, the airfoil performance drop is anticipated toward lower M values, and this is consistent with the general behavior of the lift and drag curves of Figure 7 (top). However in the transonic region a great sensitivity of the simulated pressure profile to even small variations of the actual airfoil angle of attack was evidenced, particularly as regards the supersonic bubble occurring on the suction side. This is a well renowned phenomenon in the literature of such kind of supercritical airfoils, for which the experimental uncertainty could play a dramatic role.

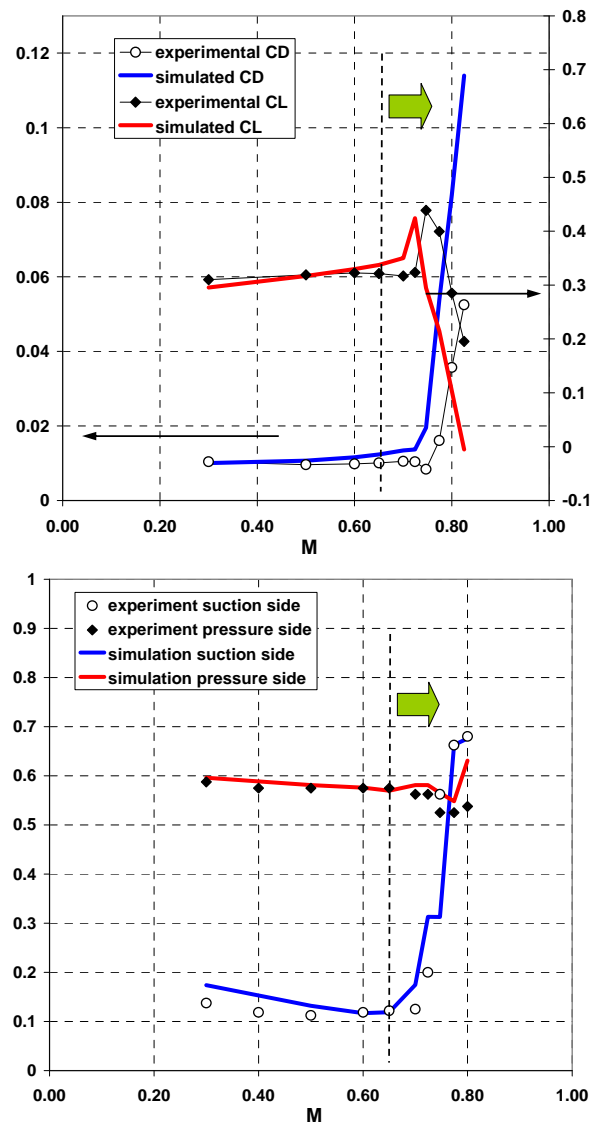


Figure 7 Lift and drag coefficients as a function of the Mach number in the range $M \geq 0.7$ (top). Location of natural laminar/turbulent transition in the range $M \geq 0.7$: comparison between experimental and computed values (bottom)

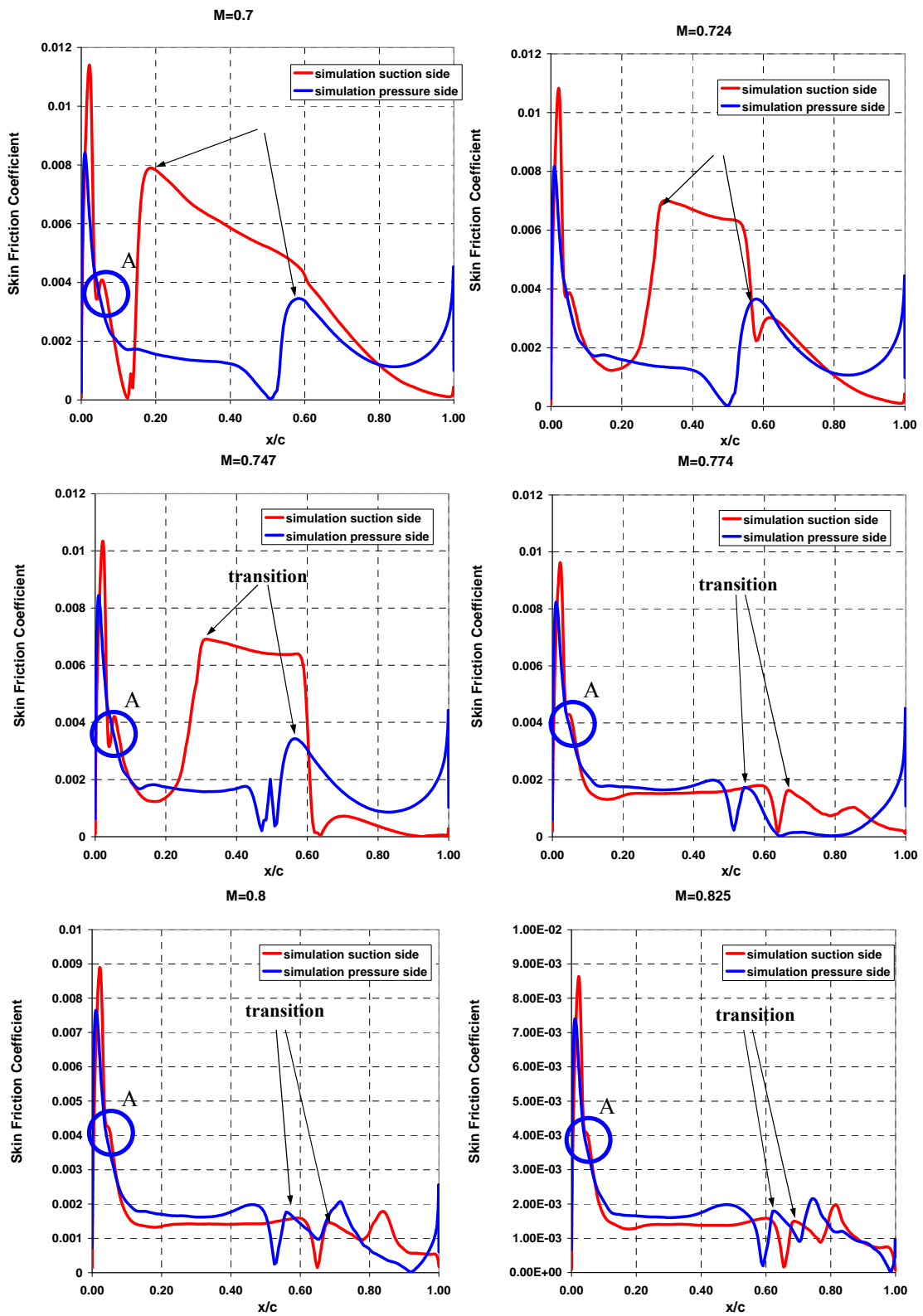


Figure 8 Skin friction coefficient distributions over the airfoil surface for $M \geq 0.7$

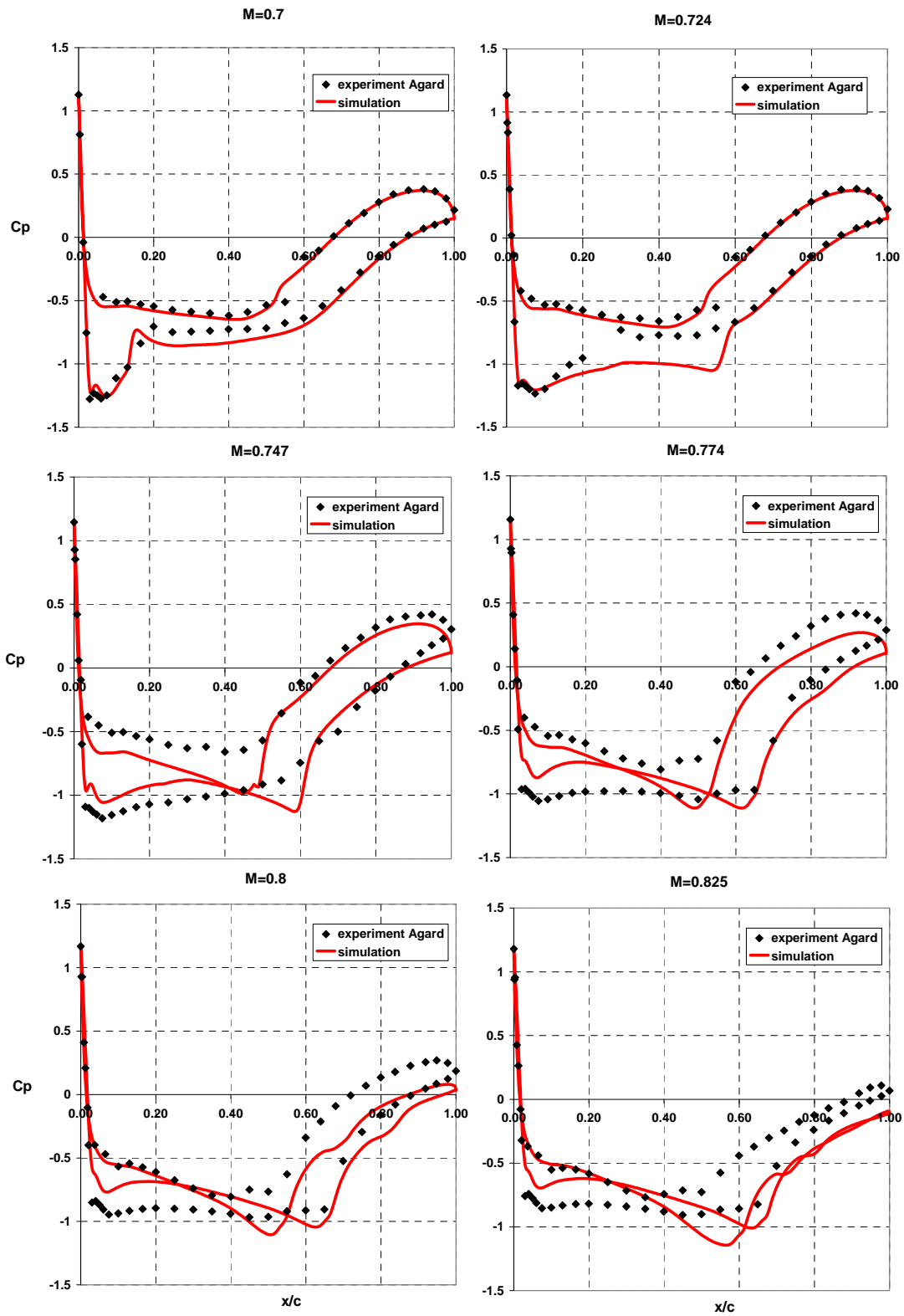


Figure 9 Pressure coefficient distributions over the airfoil surface for $M \geq 0.7$

CONCLUSIONS

At low to medium Mach number flows the transitional SST turbulence model was proved to be accurate in predicting the lift and drag coefficients and the onset of laminar/turbulent transition on both the suction and pressure sides of a rather challenging test-case airfoil (NLR 7301).

The maximum discrepancy between the predicted and experimental lift coefficient was in the order of +5% at $M=0.65$. Below this value, the error is much less and becomes about -0.5% at $M=0.5$. Regarding the drag coefficient, a very similar trend was evidenced (maximum discrepancy equal to 21% at $M=0.65$ and -3% at $M=0.3$). This is a very remarkable result, leading to a high confidence level in the calculated performance. An excellent predictive capability was also evidenced in estimating the transition point on both suction and pressure sides as the comparisons with experimental data highlight.

An important issue deserves to be underlined, in that the results obtained showed a certain degree of sensitivity to the turbulence intensity level set at the domain inlet: while pressure distribution over the airfoil remains roughly unchanged with increasing turbulence levels, the transition onset is anticipated on both sides, thus leading to a larger drag.

As the Mach number increases, the discrepancy in both the lift and drag coefficients becomes higher, but the tendency is well calculated. Prediction of transition location on both sides of the airfoil is very accurate, even if the correlation on the pressure distributions is not satisfactory.

The numerical results need however to be interpreted since the experimental data, especially those at high Mach numbers, are affected by various sources of uncertainty, as reported by other researchers [7,8]. The most relevant issue regards the influence of the actual angle of attack on the onset and spatial development of the supersonic bubble taking place on the suction side near the leading edge of the airfoil at positive attitudes. In fact, simulations revealed that the magnitude of such bubble had a remarkable influence on the shape of the pressure coefficient distribution and, therefore on the lift and drag experienced by the airfoil. As a consequence, some partially unsatisfactory correlations registered at transonic flow regimes could be attributed to inaccurate airfoil stagger angles. It is worth considering that dramatic changes in the pressure coefficient distributions, particularly towards the rear of the airfoil, occur when varying this angle even by a small fraction of degree.

REFERENCES

- [1] Menter, F. R., Langtry, R. B., Likki S. R., Suzen, Y. B., Huang, P. G., Völker, S., "A Correlation-Based Transition Model Using Local Variables — Part I: Model Formulation," *Journal of Turbomachinery*, Volume 128, Issue 3, pp. 413-422, 2006.
- [2] Menter, F. R., Langtry, R. B., Likki S. R., Suzen, Y. B., Huang, P. G., Völker, S., "A Correlation-Based Transition Model Using Local Variables — Part II: Test Cases and Industrial Applications," *Journal of Turbomachinery*, Volume 128, Issue 3, pp. 423-434, 2006.
- [3] Menter, F. R., "Two-Equation Eddy-Viscosity Turbulence Models for Engineering Applications," *AIAA Journal*, Vol. 32, No. 8, pp. 1598-1605, 1994.
- [4] Menter, F. R., "Improved Two-Equation k-omega Turbulence Models for Aerodynamic Flows," NASA TM 103975, October 1992.
- [5] Menter, F. R., Kuntz, M., Langtry, R., "Ten Years of Industrial Experience with the SST Turbulence Model," *Turbulence, Heat and Mass Transfer*, K. Hanjalic, Y. Nagano, and M. Tummers (Editors), Begell House, Inc., pp. 625 – 632, 2003.
- [6] AGARD Advisory Report N 138, "Experimental data base for computer program assessment: report of the fluid dynamics panel working group 04", January 1979.
- [7] Castro, B.M., Jones, K.D, Platzer, M.F., Weber, S. and Ekaterinaris, J.A. "Numerical Investigation of Transonic Flutter and Modeling of Wind Tunnel Interference Effects," *IUTAM Symposium Transsonicum IV*, Sobieczky. (Ed.), H., Kluwer Academic Publishers, Dordrecht, The Netherlands, 2003, pp. 71-78.
- [8] Kumar, R., Singh, N., "Unsteady Transonic Aerodynamic Analysis for Oscillatory Airfoils and Oscillating Flaps Using Dynamic Mesh", *Proceedings of the 2nd International Congress on Computational Mechanics and Simulation*, Guwahati, India, December 2006.